



ORIGINAL ARTICLE

OPEN

Head-to-head comparison of magnetic resonance elastography-based liver stiffness, fat fraction, and T1 relaxation time in identifying at-risk NASH

Jiahui Li¹  | Xin Lu^{1,2} | Zheng Zhu¹ | Kyle J. Kalutkiewicz¹ |
 Taofic Mounajjed³ | Terry M. Therneau⁴ | Sudhakar K. Venkatesh¹  | Yi Sui¹ |
 Kevin J. Glaser¹ | Safa Hoodeshenas¹ | Armando Manduca¹  | Vijay H. Shah⁵ |
 Richard L. Ehman¹  | Alina M. Allen⁵  | Meng Yin¹ 

¹Department of Radiology, Mayo Clinic, Rochester, Minnesota, USA

²Department of Radiology, Zhongshan Hospital, Fudan University, Shanghai, China

³Division of Anatomic Pathology, Mayo Clinic, Rochester, Minnesota, USA

⁴Department of Biomedical Statistics and Informatics, Mayo Clinic, Rochester, Minnesota, USA

⁵Division of Gastroenterology and Hepatology, Mayo Clinic, Rochester, Minnesota, USA

Correspondence

Meng Yin, Department of Radiology, Mayo Clinic, 200 First St SW, Rochester, Minnesota 55905, USA.

Email: yin.meng@mayo.edu

Alina M. Allen, Division of Gastroenterology and Hepatology, Mayo Clinic, 200 First St SW, Rochester, Minnesota 55905, USA.

Email: allen.alina@mayo.edu

Abstract

Background and Aims: The presence of at-risk NASH is associated with an increased risk of cirrhosis and complications. Therefore, noninvasive identification of at-risk NASH with an accurate biomarker is a critical need for pharmacologic therapy. We aim to explore the performance of several magnetic resonance (MR)-based imaging parameters in diagnosing at-risk NASH.

Approach and Results: This prospective clinical trial (NCT02565446) includes 104 paired MR examinations and liver biopsies performed in patients with suspected or diagnosed NAFLD. Magnetic resonance elastography-assessed liver stiffness (LS), 6-point Dixon-derived proton density fat fraction (PDFF), and single-point saturation-recovery acquisition-calculated T1 relaxation time were explored. Among all predictors, LS showed the significantly highest accuracy in diagnosing at-risk NASH [AUC_{LS}: 0.89 (0.82, 0.95), AUC_{PDFF}: 0.70 (0.58, 0.81), AUC_{T1}: 0.72 (0.61, 0.82), z-score test $z > 1.96$ for LS vs any of others]. The optimal cutoff value of LS to identify at-risk NASH patients was 3.3 kPa (sensitivity: 79%, specificity: 82%, negative predictive value: 91%), whereas the optimal cutoff value of T1 was 850 ms (sensitivity: 75%, specificity: 63%, and negative predictive value: 87%). PDFF had the highest performance in diagnosing NASH with any fibrosis stage [AUC_{PDFF}: 0.82 (0.72, 0.91), AUC_{LS}: 0.73 (0.63, 0.84), AUC_{T1}: 0.72 (0.61, 0.83), $|z| < 1.96$ for all].

Abbreviations: BMI, body mass index; cT1, corrected T1; LS, liver stiffness; MRE, magnetic resonance elastography; NPV, negative predictive value; PDFF, proton density fat fraction; PPV, positive predictive value; ROI, regions of interest.

Jiahui Li and Xin Lu are co-first authors.

Supplemental Digital Content is available for this article. Direct URL citations are provided in the HTML and PDF versions of this article on the journal's website, www.hepjournal.com.

This is an open access article distributed under the terms of the Creative Commons Attribution-Non Commercial-No Derivatives License 4.0 (CCBY-NC-ND), where it is permissible to download and share the work provided it is properly cited. The work cannot be changed in any way or used commercially without permission from the journal.

Copyright © 2023 The Author(s). Published by Wolters Kluwer Health, Inc.

Conclusion: Magnetic resonance elastography-assessed LS alone outperformed PDFF, and T1 in identifying patients with at-risk NASH for therapeutic trials.

INTRODUCTION

NAFLD is a worldwide epidemic with increasing prevalence.^[1] As the progressive form of NAFLD, NASH accounts for the increase in cirrhosis since 1990.^[2] Fibrosis is the most important predictor of mortality in NAFLD.^[3] It has been demonstrated that patients with NASH with fibrosis, particularly stage 2 or higher, have less favorable outcomes with a significantly increased risk of liver-related mortality.^[4–7] A NASH diagnosis with fibrosis stage 2 or higher (referred to as at-risk NASH) is now used as criteria for enrollment in clinical trials and pharmacologic therapy. Therefore, identifying patients with NASH and at-risk NASH is critically needed in clinical trials and practice.

Even though liver biopsy is currently the clinical gold standard for diagnosing NASH and fibrosis, noninvasive imaging biomarkers provide accurate quantitative assessments in monitoring disease progression/regression and evaluating therapy responses in a more practical way. Magnetic resonance elastography (MRE)-assessed liver stiffness (LS) has been demonstrated to be the most accurate noninvasive biomarker for staging fibrosis^[8–10] and a potential predictor for diagnosing NASH.^[11] Proton density fat fraction (PDFF) is a reliable biomarker for quantifying hepatic fat content, which is more sensitive and accurate than histopathological steatosis grading from liver biopsy.^[12,13] A recent meta-analysis assessed the clinical utility of iron-corrected T1 “(cT1)” in identifying patients with at-risk NASH.^[14] However, histology data derived from multiple centers were not centrally interpreted, which increases the risk of inaccurate NASH diagnosis.^[15] Therefore, we aimed to perform a single-center head-to-head comparison of the diagnostic performance of MRE-assessed LS, PDFF, and T1, in identifying patients with NASH and at-risk NASH.

METHODS

Study design and participants

This was a prospective clinical trial (NCT02565446),^[16] including 89 patients who had suspected or diagnosed NAFLD, without other known chronic liver diseases or any causes of secondary hepatic fat accumulation. All patients underwent MRI/MRE exams and liver biopsies (see the flow chart of patient enrollment in Supplemental Material S1, <http://links.lww.com/HEP/H132>).

Informed consent in writing was obtained from each patient and the study protocol conformed to the ethical guidelines of the 1975 Declaration of Helsinki as reflected in a priori approval by the Mayo Clinic Institutional Review Board.

MRI and processing

All MRI/MRE examinations were performed on 1.5T whole-body scanners (GE Healthcare) at Mayo Clinic. All patients were scanned in the supine position after a fasting period of at least 4 hours. The imaging protocol contains MRE imaging (60 Hz gradient-echo 2-dimensional MRE), 6-point Dixon imaging (IDEAL-IQ), and T1 mapping (SMART₁Map). Imaging parameters are illustrated in Supplemental Table S2, (<http://links.lww.com/HEP/H132>).

Magnetic resonance elastography

The MRE images were acquired by placing a passive driver against the anterior body wall of patients over the right lobe of the liver. The driver was held in place by an elastic band wrapped around the body. The continuous mechanical waves for MRE were generated by an active driver (Resoundant, Inc.) outside the scanner room, and were delivered to the passive driver through a 7.6 m long plastic tube. The LS measurements were calculated from freehand regions of interest drawn on each slice, which included only liver parenchyma, and avoided large vessels, bile ducts, and regions with an inadequate magnitude of signal or shear wave amplitude (ie, artifacts from cardiac movement and edges). In this study, LS represents the magnitude of the complex shear modulus ($|G^*|$) derived from 2-dimensional MRE data. It was reported as mean and SD as described in the previous study.^[17] One analyst (Jiahui Li with 5 years of experience) postprocessed all the images while blinded to clinical, laboratory, and histopathological data.

Proton density fat fraction

A 6-echo Dixon method was used to acquire the measurement of the hepatic fat fraction. Water and fat images, PDFF, and R2* (1/T2*, the relaxation rates of observable or effective T2) maps were obtained from

image reconstruction (IDEAL-IQ, GE Healthcare). The measurements of PDFF and $R2^*$ were calculated from regions of interest manually drawn in 9 anatomic segments by 2 analysts (Jiahui Li with 5 years of experience and Xin Lu with 2 years of experience), respectively.

T1 mapping

The investigational pulse sequence using single-point, saturation-recovery fast imaging using steady-state acquisition, was performed to measure the native (noncontrast) true T1 relaxation time of liver tissue. One oval-shaped regions of interest was drawn on each slice by 1 analyst (Safa Hoodeshenas, 4 years of experience), to cover as much liver parenchyma as possible, and avoid large vessels, bile ducts, fissures, and fossae. The T1 measurements were calculated as an area-weighted mean value.

Histologic assessment

All participants had liver biopsies, and 1 pathologist with expertise in NASH (Taofic Mounajjed, 10 years of experience) reviewed all the specimens while blinded to imaging, clinical and laboratory results. The histologic assessment included the presence of NASH, grade of steatosis, inflammation, ballooning, and fibrosis stage based on NASH Clinical Research Network criteria.^[18] At-risk NASH was defined as NASH with stage ≥ 2 fibrosis.

Statistical analyses

The nonparametric Dunn multiple comparison tests with Bonferroni adjustment and Wilcoxon rank sum test were applied to test the differences in imaging parameters (LS, PDFF, and T1). Spearman correlations were used to analyze the relationship between imaging biomarkers. The prediction models were generated from 3 predictors, individually or by combinations. Nominal logistic models trained with ridge regularization and iterative leave-one-out cross-validation were used to detect NASH and at-risk NASH. The overall diagnostic accuracies (reported as the AUC) of imaging prediction models were analyzed by concordance analysis using a robust variance estimator—the Huber sandwich estimator—which effectively accounts for the within-subject correlation in 15 patients with follow-up examinations/biopsies. Z-score tests were used to compare AUCs.^[19] Final retraining of each model was performed on the whole data set to estimate the standardized predictor ORs to compare predictor importance. Sensitivity, specificity, positive predictive value, and negative predictive value (NPV) were calculated to assess the predictor performance. A significance level of $p < 0.05$ for group comparisons and correlation analyses, and $|z| > 1.96$ for performance comparisons were used in this study. All statistical analyses were performed using R (survival package, version 4.1.1) and Python (version 3.8.5).

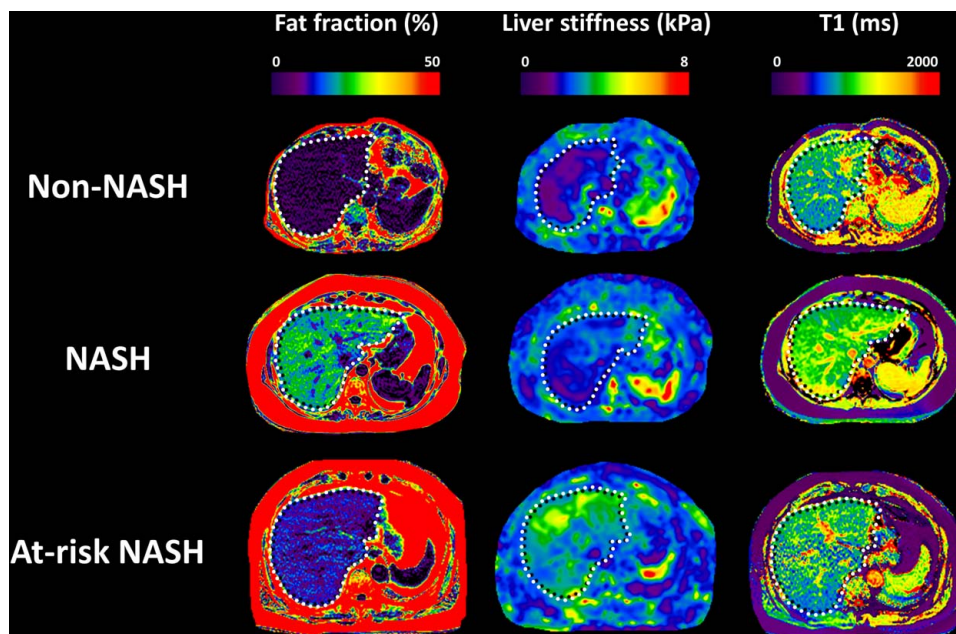


FIGURE 1 Example images. The first row represents images from a patient with non-NASH (female, 45 y, BMI = 30.2 kg/m²): PDFF = 2.1%, LS = 1.69 kPa, T1 = 794 ms. The second row represents images from a patient with NASH (female, 48 y, BMI = 32.8 kg/m²): PDFF = 20.4%, LS = 2.43 kPa, T1 = 1004 ms. The third row represents images from a patient with at-risk NASH (male, 60 y, BMI = 27.5 kg/m²): PDFF = 10.6%, LS = 3.94 kPa, T1 = 858 ms. The white dotted line illustrates the contour of the liver not the ROI for measurements. Abbreviations: BMI, body mass index; LS, liver stiffness; ROI, regions of interest; PDFF, proton density fat fraction.

RESULTS

Patient characteristics

In this prospective clinical trial (NCT02565446), we enrolled 89 participants at risk of NAFLD, who underwent a total of 104 MRI/MRE examinations paired with concurrent liver biopsy. The purpose of these procedures was to evaluate the diagnostic accuracy of various imaging parameters in the longitudinal monitoring of NAFLD. Of the 104 MRI/MRE examinations, 89 were performed at baseline/enrollment and 15 examinations were performed after 1-year follow-up. During the time between the two assessments, 2 participants underwent a bariatric operation, whereas the remaining 13 received lifestyle counseling but did not receive any medication treatment. The NAFLD activity score changed in 9 of the 15 patients between the two assessments, thus they were accounted as 2 independent assessments. The median time between MRI/MRE and liver biopsy was 1 day (interquartile range: 1, 7). Among the 104 paired examinations, 45 (43%) were diagnosed with NASH and 28 (27%) were identified as at-risk NASH by histology (example images shown in [Figure 1](#)). [Table 1](#) represents the participant characteristics.

Performance of proton density fat fraction and T1 in diagnosing steatosis and NASH

As shown in [Figure 2](#), both PDFF and T1 showed a significant increase in values as the severity of steatosis increased (Kruskal-Wallis rank sum test, $p < 0.0001$ for both). Patients with NASH had significantly elevated PDFF [18.5% (12.5, 23.2) vs 6.0% (3.5, 11.5), $p < 0.0001$] and T1 [901 ms (818.6, 1016.6) vs 809.4 ms (746.0, 885.7), $p = 0.0002$] when compared with non-NASH patients.

Performance of liver stiffness and T1 in diagnosing fibrosis and at-risk NASH

Both LS and T1 values were higher in patients with clinically significant fibrosis (stage ≥ 2) [LS: 4.1 kPa (3.4, 6.1) vs 2.3 kPa (2.0, 2.6), $p < 0.0001$; T1: 890.6 ms (808.1, 995.1) vs 821.3 ms (745.0, 924.6), $p = 0.008$], and at-risk NASH [LS: 3.9 kPa (3.3, 6.1) vs 2.4 kPa (2.1, 2.8), $p < 0.0001$; T1: 925.1 ms (847.2, 1019.7) vs 817.9 ms (746.5, 927.0), $p = 0.0008$] ([Figure 3](#)).

T1 significantly correlated with PDFF ($R = 0.62$, $p < 0.01$), whereas LS did not show any correlation with PDFF ($R = 0.03$, $p = 0.77$) ([Figure 4](#)).

TABLE 1 Demographic, histologic, and imaging characteristics of participants

Characteristics	Paired examinations (N = 104) in 89 participants; n (%)
General information	
Time interval between MRI/MRE and liver biopsy (d)	1 (1, 7)
Sex (F)	64 (62)
Age (y)	55 (46, 60)
BMI (kg/m ²)	33 (30, 39)
Diabetes (yes)	48 (46)
Histologic findings	
Steatosis grade	
0	31 (30)
1	47 (45)
2	22 (21)
3	4 (4)
Lobular inflammation grade	
0	43 (41)
1	57 (55)
2	4 (4)
Ballooning grade	
0	59 (57)
1	32 (31)
2	13 (13)
Fibrosis stage	
0	54 (52)
1	12 (12)
2	13 (13)
3	11 (11)
4	14 (13)
NASH	45 (43)
At-risk NASH	28 (27)
Imaging findings	
LS (kPa)	2.7 (2.1, 3.7)
PDFF (%)	10.6 (5.4, 19.7)
T1 relaxation time (ms)	843.9 (765.7, 967.3)
R2* (s ⁻¹)	37.2 (35.0, 41.3)

Note: Continuous measurements are reported as median (interquartile range). Discrete variables are reported as the number and proportion of subjects with the characteristics of interest. All data were calculated regarding each independent examination with paired imaging and biopsy. Abbreviations: BMI, body mass index; LS, liver stiffness; MRE, magnetic resonance elastography; PDFF, proton density fat fraction.

Diagnostic accuracy in identifying patients with NASH and at-risk NASH

We evaluated the diagnostic performance of several logistic regression models with imaging predictors in identifying patients with NASH and

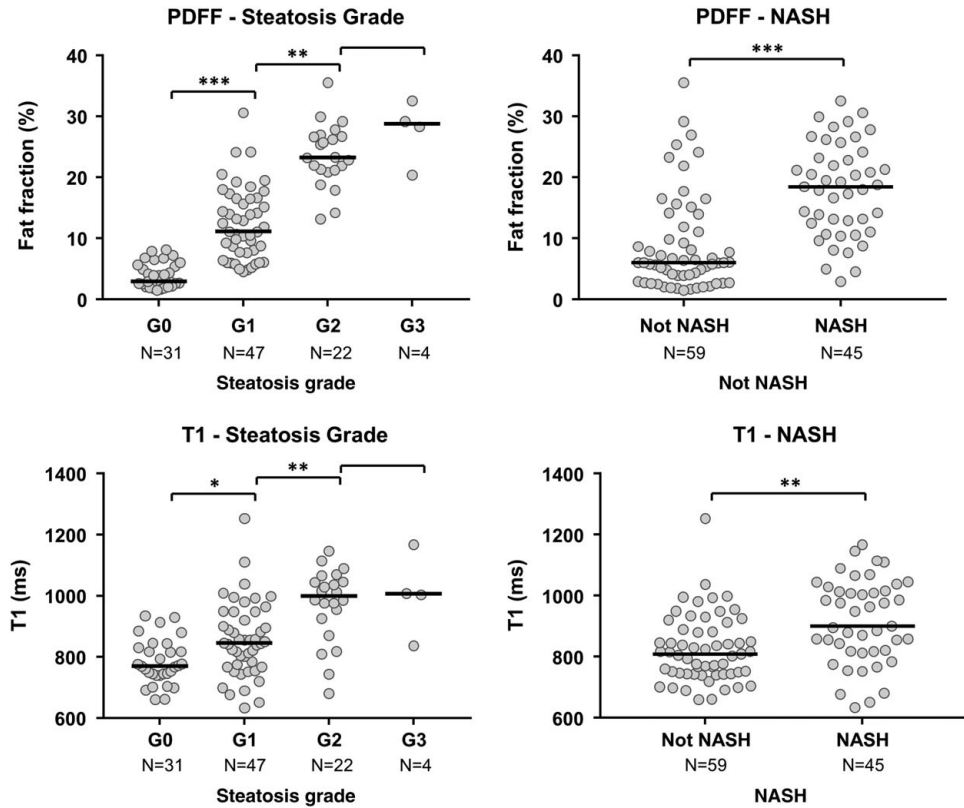


FIGURE 2 Scatter plots of PDFF and T1 for differentiating steatosis grades and NASH. The black line indicates the median value. * $p < 0.05$; ** $p < 0.01$; *** $p < 0.0001$. Abbreviation: PDFF, proton density fat fraction.

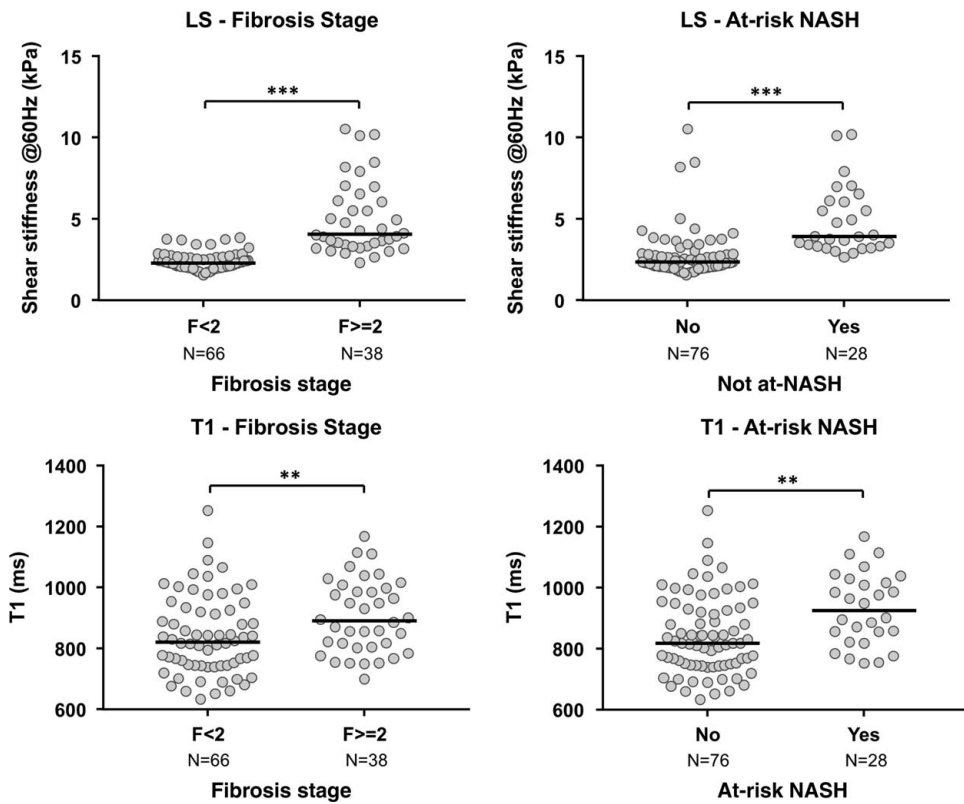


FIGURE 3 Scatter plots of LS and T1 for differentiating clinically significant fibrosis (\geq stage 2) and at-risk NASH. The black line indicates the median value. * $p < 0.05$; ** $p < 0.01$; *** $p < 0.0001$. Abbreviation: LS, liver stiffness.

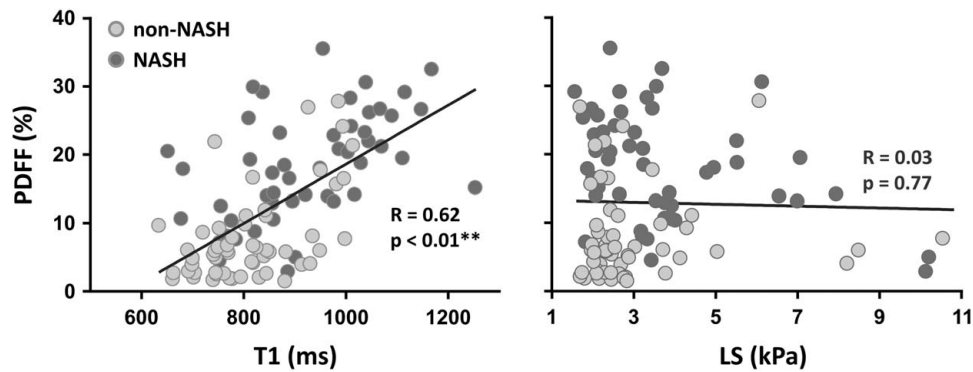


FIGURE 4 Correlations between PDFF and T1/LS. $^{**}p < 0.01$. Abbreviations: LS, liver stiffness; PDFF, proton density fat fraction.

at-risk NASH (Figure 5). The multivariate model of PDFF + LS + T1 showed the highest AUC value (0.83, 95% CI: 0.75, 0.92) in diagnosing NASH. The univariable model of LS showed the highest AUC value (0.89, 95% CI: 0.82, 0.95) in diagnosing at-risk NASH.

PDFF showed the most significant effect (ie, highest standardized ORs) in all univariable and multivariable models for diagnosing patients with NASH. Similarly, LS showed the most significant impact in diagnosing patients with at-risk NASH (Table 2).

The optimal cutoff value of LS to identify patients with at-risk NASH was 3.3 kPa, with a sensitivity of 79%, a specificity of 82%, and an NPV of 91%. The optimal cutoff value of T1 was 850 ms, with a sensitivity of 75%, a specificity of 63%, and an NPV of 87% (Table 3).

When evaluated in those with and without diabetes, the diagnostic performance of the imaging parameters was similar, although the CIs for the AUC were larger due to the decrease in sample sizes of the 2 groups.

DISCUSSION

In this prospective study, we directly compared LS, PDFF, T1, and 4 multiparametric models of MRI/MRE parameters for the detection of NASH and at-risk NASH.

To our knowledge, this is the head-to-head comparison study on the performance of LS, PDFF, and T1 for NASH

and at-risk NASH. MRE-assessed LS is a well-established most accurate imaging biomarker for diagnosing clinically significant fibrosis.^[20] In this analysis, LS alone showed the highest diagnostic accuracy in identifying at-risk NASH [AUC: 0.89 (0.82, 0.95)]. The inferior performance of the models with additional parameters to LS is likely due to collinearity or nonlinear relationship between steatosis and NAFLD severity,^[21,22] described as “burnt-out” NASH (Supplemental Figure S3, <http://links.lww.com/HEP/H132>). In contrast, the LS is known to monotonically increase with fibrosis,^[23] inflammation,^[24] and ballooning,^[25] which are all hallmark histopathologic features of at-risk NASH.

Consistent with previous studies, T1 correlated with hepatic steatosis and fibrosis.^[26,27] Compared with LS or PDFF, however, T1 was inferior in diagnosing patients with at-risk NASH or NASH, respectively. A recent meta-analysis of multicenter pooled data assessed the clinical utility of PDFF and cT1, for identifying patients with NASH and at-risk NASH.^[14] The diagnostic performance for identifying NASH was similar (AUC_{cT1} : 0.78 vs AUC_{PDFF} : 0.78). For at-risk NASH diagnosis, cT1 outperformed PDFF in the pooled analysis (AUC_{cT1} : 0.78 vs AUC_{PDFF} : 0.69, $p < 0.001$), whereas in individual patient data meta-analysis, the performance of cT1 was inferior (AUC_{cT1} : 0.73 vs AUC_{PDFF} : 0.69). Notably, there was significant heterogeneity across sites, with one site ($n = 26$) reporting AUC 0.57 (0.27, 0.87) for cT1 in diagnosing at-risk NASH. Technically, the single-point saturation-recovery

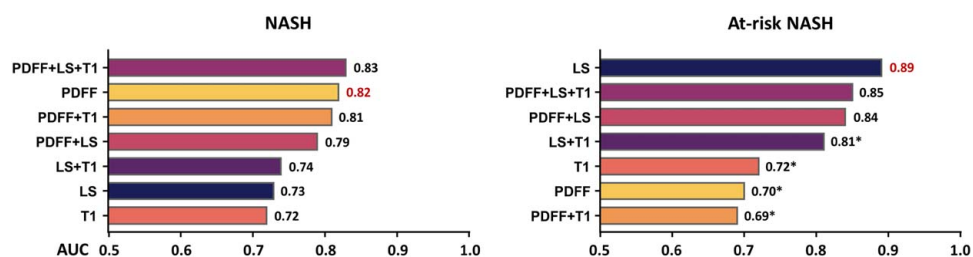


FIGURE 5 Summary of AUC for nominal logistic models for distinguishing NASH and at-risk NASH. $^*z > 1.96$ when compared with LS in diagnosing at-risk NASH. Abbreviations: LS, liver stiffness; PDFF, proton density fat fraction.

TABLE 2 Univariate and multivariate prediction models in diagnosing NASH and at-risk NASH

Predictors	Univariate		PDFF + LS		PDFF + T1		LS + T1		PDFF + LS + T1	
	Coefficient	OR	Coefficient	OR	Coefficient	OR	Coefficient	OR	Coefficient	OR
NASH										
PDFF	0.08	1.97	0.15	3.98	0.08	2.05	—	—	0.20	6.02
LS	0.33	1.86	0.44	2.28	—	—	0.27	1.67	0.45	2.35
T1	0.00	1.88	—	—	0.00	0.86	0.00	1.14	0.00	0.54
At-risk NASH										
PDFF	0.04	1.47	0.06	1.71	0.05	1.51	—	—	0.11	2.65
LS	0.87	5.25	0.55	2.85	—	—	0.87	5.21	0.92	5.75
T1	0.01	2.13	—	—	0.00	1.48	0.00	1.60	0.00	0.82

Abbreviations: LS, liver stiffness; PDFF, proton density fat fraction.

Bold values indicate highest standardized ORs.

acquisition method has been shown to provide more accurate and robust T1 measurements than the MOLLI method (cT1)^[28,29] (detailed information for T1 and cT1 could be found in Supplemental Material S4, <http://links.lww.com/HEP/H132>). Both cT1 and T1 measure a mixed signal from water and fat in the liver,^[30,31] and have a potential bias from the partial volume effect of steatosis.^[32] Consequently, T1 is significantly associated with PDFF measurements in NAFLD/NASH.^[30] Therefore, the inferior performance of T1 in diagnosing NASH and at-risk NASH observed in this study is likely due to signal confounders and collinearity with the other biomarkers.

Cost is an important consideration in the application of imaging-based biomarkers. An MRI examination consisting of MRE alone or MRE with PDFF is much less expensive than the procedure for obtaining cT1 and PDFF. To obtain a measurement of liver cT1, an MRI procedure is performed using a proprietary protocol and the data must be sent for external processing for an extra cost. According to the US Centers for Medicaid and Medicare Services, the relevant charges are ~\$350 (MRI abdomen without contrast, CPT code 74181) and \$950 (quantitative MR tissue analysis, CPT code

0648T), for a total of ~\$1300 (which would include a PDFF measurement). The Centers for Medicaid and Medicare Services charge for MRE is ~\$240 (CPT code 76391). The acquisition for PDFF requires only a single breath-hold and could be included in the MRE examination at no additional charge. Even if it is charged as an “abdomen without contrast” (CPT code 74181), the total Centers for Medicaid and Medicare Services charge for MRE + PDFF would be less than half that for cT1 + PDFF.

Similarly, cost-effectiveness studies with nonimaging biomarkers are warranted. Many studies demonstrated that MRE-assessed LS is superior in stratifying at-risk NASH compared with NIS4 [AUC: 0.80 (0.77, 0.84)],^[33] FAST (FibroScan-Aspartate aminotransferase) score [AUC: 0.80 (0.76, 0.85)],^[34] and LAD-NASH (predictive model with US markers of liver stiffness, attenuation coefficient, and dispersion slope) score [AUC: 0.86 (0.79, 0.93)].^[35]

There are several strengths of this study. As the head-to-head comparison study, the number of paired examinations (N = 104) is sufficiently large. The post hoc power analysis for group comparisons is over 89%. Furthermore, for all 104 examinations with paired concurrent biopsy, the median time

TABLE 3 Diagnostic accuracy of LS and T1 to diagnose patients with at-risk NASH at prespecified thresholds

AUC	Threshold	Sensitivity (%)	Specificity (%)	NPV (%)	PPV (%)
LS; 0.89 (95% CI: 0.82-0.95) (kPa)	≥ 2.9	96	79	98	63
	≥ 3.1	89	80	95	63
	≥ 3.3	79	82	91	61
	≥ 3.5	68	84	88	61
	≥ 3.7	57	86	84	59
T1; 0.72 (95% CI: 0.61-0.82) (ms)	≥ 750	100	28	100	34
	≥ 800	82	41	86	34
	≥ 850	75	63	87	43
	≥ 900	54	71	81	41
	≥ 950	46	80	80	46

Abbreviations: LS, liver stiffness; NPV, negative predictive value; PPV, positive predictive value.

interval is very short [1 d (1, 7)], which provided reliable histology information. Centralized data collection and processing avoided interobserver bias in histologic interpretation. Several limitations are worth noting. First, this is a single-center study, without external validation. To mitigate this limitation, the model performance was calculated using leave-one-out cross-validation methods. Second, there were 15 participants who underwent 2 examinations/biopsies 1 year apart. To mitigate potential bias related to measurements in the same participant, concordance analysis with a robust variance estimator was performed to correct the within-subject correlation. The diagnostic performance of models in 89 participants without repeated examinations showed similar results as the original analysis (Supplemental Figure and Table S5, Supplemental Digital Content 1, <http://links.lww.com/HEP/H132>). Third, the sample size is relatively small, with only 28 (27%) out of 104 examinations having at-risk NASH by histology, when most patients had mild liver disease with low inflammation and ballooning grade. Nevertheless, this reflects the real-world prevalence of at-risk NASH and enables the generalization of these results, including the positive predictive value and NPV for clinical practice.^[36] These results should be validated in multicenter cohorts with larger sample sizes.

In conclusion, this study demonstrates that among the imaging biomarkers evaluated, MRE-assessed LS has the highest accuracy for identifying at-risk NASH. Therefore, MRE is the most accurate test to identify patients with NASH and stage 2–3 fibrosis or cirrhosis who may qualify for drug therapies in clinical trials and practice once approved.

AUTHOR CONTRIBUTIONS

Study design, database creation, and data acquisition: Jiahui Li, Xin Lu, and Zheng Zhu. Manuscript preparation: Jiahui Li, Xin Lu, Alina M. Allen, and Meng Yin. Statistical analysis: Jiahui Li and Kyle J. Kalutkiewicz. Statistical review: Terry M. Therneau. Critical revision of the manuscript: Jiahui Li, Terry M. Therneau, Richard L. Ehman, Alina M. Allen, and Meng Yin. Imaging review: Safa Hoodeshenas, Sudhakar K. Venkatesh, and Taofic Mounajjed. Technical/material support: Yi Sui, Kevin J. Glaser, Armando Manduca, Sudhakar K. Venkatesh, Vijay H. Shah, Richard L. Ehman, Alina M. Allen, and Meng Yin. Study concept and design, database creation, funding obtainment, and study supervision: Vijay H. Shah, Richard L. Ehman, Alina M. Allen, and Meng Yin.







FUNDING INFORMATION

This work has been supported by grant funding from the National Institutes of Health (K23 DK115594, P30 DK084567, R01 AA021171, R37 EB001981, R01 EB017197), the US Department of Defense (W81XWH-19-1-0583-01), and the Mayo Clinic.

CONFLICTS OF INTEREST

Kyle J. Kalutkiewicz is employed by and consults for Resoundant, Inc. Kevin J. Glaser owns stock in and intellectual property rights with Resoundant, Inc. Armando Manduca owns stock in Resoundant, Inc. Richard L. Ehman owns stock in, owns intellectual property rights with, and received grants from Resoundant, Inc. Alina M. Allen consults for, advises, and received grants from Novo Nordisk. She received grants from Pfizer and Target Pharma. Meng Yin owns stock in and intellectual property rights with Resoundant, Inc. The remaining authors have no conflicts to report.

ORCID

Jiahui Li  <https://orcid.org/0000-0002-4889-0714>
 Sudhakar K. Venkatesh  <https://orcid.org/0000-0002-7514-1030>
 Armando Manduca  <https://orcid.org/0000-0002-9411-5671>
 Richard L. Ehman  <https://orcid.org/0000-0001-7041-5074>
 Alina M. Allen  <https://orcid.org/0000-0002-8393-8410>
 Meng Yin  <https://orcid.org/0000-0001-6778-192X>

REFERENCES

- Paik JM, Golabi P, Younossi Y, Srishord M, Mishra A, Younossi ZM. The growing burden of disability related to nonalcoholic fatty liver disease: Data from the global burden of disease 2007–2017. *Hepatol Commun*. 2020;4:1769–80.
- Sepanlou SG, Safiri S, Bisignano C, Ikuta KS, Merat S, Saberifiroozi M, et al. The global, regional, and national burden of cirrhosis by cause in 195 countries and territories, 1990–2017: a systematic analysis for the Global Burden of Disease Study 2017. *Lancet Gastroenterol Hepatol*. 2020;5:245–66.
- Simon TG, Roelstraete B, Khalili H, Hagström H, Ludvigsson JF. Mortality in biopsy-confirmed nonalcoholic fatty liver disease: results from a nationwide cohort. *Gut*. 2021;70:1375–82.
- Kleiner DE, Brunt EM, Wilson LA, Behling C, Guy C, Contos M, et al. Association of histologic disease activity with progression of non-alcoholic fatty liver disease. *JAMA Netw Open*. 2019;2:e1912565.
- Rowe IA, Parker R. The diagnosis of nonalcoholic fatty liver disease should carry important prognostic information. *Nat Rev Gastroenterol Hepatol*. 2019;16:449–50.
- Dulai PS, Singh S, Patel J, Soni M, Prokop LJ, Younossi Z, et al. Increased risk of mortality by fibrosis stage in nonalcoholic fatty liver disease: Systematic review and meta-analysis. *Hepatology*. 2017;65:1557–65.
- Ekstedt M, Hagström H, Nasr P, Fredrikson M, Stål P, Kechagias S, et al. Fibrosis stage is the strongest predictor for disease-specific mortality in NAFLD after up to 33 years of follow-up. *Hepatology*. 2015;61:1547–54.
- Singh S, Venkatesh SK, Wang Z, Miller FH, Motosugi U, Low RN, et al. Diagnostic performance of magnetic resonance elastography in staging liver fibrosis: a systematic review and meta-analysis of individual participant data. *Clin Gastroenterol Hepatol*. 2015;13:440–51 e446.
- Idilman IS, Li J, Yin M, Venkatesh SK. MR elastography of liver: current status and future perspectives. *Abdom Radiol (NY)*. 2020;45:3444–62.
- Selvaraj EA, Mózes FE, Jayaswal ANA, Zafarmand MH, Vali Y, Lee JA, et al. Diagnostic accuracy of elastography and magnetic

- resonance imaging in patients with NAFLD: A systematic review and meta-analysis. *J Hepatol.* 2021;75:770–85.
11. Dzyubak B, Li J, Chen J, Mara KC, Therneau TM, Venkatesh SK, et al. Automated Analysis of multiparametric magnetic resonance imaging/magnetic resonance elastography exams for prediction of nonalcoholic steatohepatitis. *J Magn Reson Imaging.* 2021;54:122–31.
 12. Nouredin M, Lam J, Peterson MR, Middleton M, Hamilton G, Le TA, et al. Utility of magnetic resonance imaging versus histology for quantifying changes in liver fat in nonalcoholic fatty liver disease trials. *Hepatology.* 2013;58:1930–40.
 13. Troelstra MA, Witjes JJ, van Dijk AM, Mak AL, Gurney-Champion O, Runge JH, et al. Assessment of imaging modalities against liver biopsy in nonalcoholic fatty liver disease: The Amsterdam NAFLD-NASH cohort. *J Magn Reson Imaging.* 2021;54:1937–49.
 14. Andersson A, Kelly M, Imajo K, Nakajima A, Fallowfield JA, Hirschfeld G, et al. Clinical utility of MRI biomarkers for identifying NASH patients at high risk of progression: a multicenter pooled data and meta-analysis. *Clin Gastroenterol Hepatol.* 2022;20:2451–461.e3.
 15. Pournik O, Alavian SM, Ghalichi L, Seifizarei B, Mehrmouh L, Aslani A, et al. Inter-observer and intra-observer agreement in pathological evaluation of non-alcoholic fatty liver disease suspected liver biopsies. *Hepat Mon.* 2014;14:e15167.
 16. ClinicalTrials.gov. Transforming Non-Invasive Liver Disease Detection by MRE: The Hepatogram. 2015. Accessed May 11, 2023. <https://ClinicalTrials.gov/show/NCT02565446>.
 17. Manduca A, Bayly PJ, Ehman RL, Kolipaka A, Royston TJ, Sack I, et al. MR elastography: Principles, guidelines, and terminology. *Magn Reson Med.* 2021;85:2377–90.
 18. Kleiner DE, Brunt EM, Van Natta M, Behling C, Contos MJ, Cummings OW, et al. Design and validation of a histological scoring system for nonalcoholic fatty liver disease. *Hepatology.* 2005;41:1313–21.
 19. Kang L, Chen W, Petrick NA, Gallas BD. Comparing two correlated C indices with right-censored survival outcome: a one-shot nonparametric approach. *Stat Med.* 2015;34:685–703.
 20. Zhang YN, Fowler KJ, Boehringer AS, Montes V, Schlein AN, Covarrubias Y, et al. Comparative diagnostic performance of ultrasound shear wave elastography and magnetic resonance elastography for classifying fibrosis stage in adults with biopsy-proven nonalcoholic fatty liver disease. *Eur Radiol.* 2022;32:2457–69.
 21. Wildman-Tobriner B, Middleton MM, Moylan CA, Rossi S, Flores O, Chang ZA, et al. Association between magnetic resonance imaging-proton density fat fraction and liver histology features in patients with nonalcoholic fatty liver disease or nonalcoholic steatohepatitis. *Gastroenterology.* 2018;155:1428–35.e1422.
 22. Dennis A, Kelly MD, Fernandes C, Mouchti S, Fallowfield JA, Hirschfeld G, et al. Correlations between MRI biomarkers PDFF and cT1 with histopathological features of non-alcoholic steatohepatitis. *Front Endocrinol.* 2021;11:575843.
 23. Chen J, Allen AM, Therneau TM, Chen J, Li J, Hoodeshenas S, et al. Liver stiffness measurement by magnetic resonance elastography is not affected by hepatic steatosis. *Eur Radiol.* 2022;32:950–8.
 24. Li J, Allen AM, Shah VH, Manduca A, Ehman RL, Yin M. NAFLD MR Imaging Research Group. Longitudinal changes in MR elastography-based biomarkers in obese patients treated with bariatric surgery. *Clin Gastroenterol Hepatol.* 2023;21:220–22.e3.
 25. Imajo K, Tetlow L, Dennis A, Shumbayawonda E, Mouchti S, Kendall TJ, et al. Quantitative multiparametric magnetic resonance imaging can aid non-alcoholic steatohepatitis diagnosis in a Japanese cohort. *World J Gastroenterol.* 2021;27:609–23.
 26. Ahn JH, Yu JS, Park KS, Kang SH, Huh JH, Chang JS, et al. Effect of hepatic steatosis on native T1 mapping of 3T magnetic resonance imaging in the assessment of T1 values for patients with non-alcoholic fatty liver disease. *Magn Reson Imaging.* 2021;80:1–8.
 27. Li Z, Sun J, Hu X, Huang N, Han G, Chen L, et al. Assessment of liver fibrosis by variable flip angle T1 mapping at 3.0T. *J Magn Reson Imaging.* 2016;43:698–703.
 28. Slavin GS, Stainsby JA. True T1 mapping with SMART(1)Map (saturation method using adaptive recovery times for cardiac T (1) mapping): a comparison with MOLLI. *J Cardiovasc Magn Reson.* 2013;15(suppl 1):P3.
 29. Stainsby JA, Slavin GS. Comparing the accuracy and precision of SMART1Map, SASHA and MOLLI. *J Cardiovasc Magn Reson.* 2014;16:P11.
 30. Erden A, Kuru Öz D, Peker E, Kul M, Özalp Ateş FS, Erden İ, et al. MRI quantification techniques in fatty liver: the diagnostic performance of hepatic T1, T2, and stiffness measurements in relation to the proton density fat fraction. *Diagn Interv Radiol.* 2021;27:7–14.
 31. Mojtahed A, Kelly CJ, Herlihy AH, Kin S, Wilman HR, McKay A, et al. Reference range of liver corrected T1 values in a population at low risk for fatty liver disease—a UK Biobank sub-study, with an appendix of interesting cases. *Abdominal Radiol.* 2019;44:72–84.
 32. Kellman P, Bandettini WP, Mancini C, Hammer-Hansen S, Hansen MS, Arai AE. Characterization of myocardial T1-mapping bias caused by intramyocardial fat in inversion recovery and saturation recovery techniques. *J Cardiovasc Magn Reson.* 2015;17:33.
 33. Harrison SA, Ratzliff V, Boursier J, Francque S, Bedossa P, Majd Z, et al. A blood-based biomarker panel (NIS4) for non-invasive diagnosis of non-alcoholic steatohepatitis and liver fibrosis: a prospective derivation and global validation study. *Lancet Gastroenterol Hepatol.* 2020;5:970–85.
 34. Newsome PN, Sasso M, Deeks JJ, Paredes A, Boursier J, Chan WK, et al. FibroScan-AST (FAST) score for the non-invasive identification of patients with non-alcoholic steatohepatitis with significant activity and fibrosis: a prospective derivation and global validation study. *Lancet Gastroenterol Hepatol.* 2020;5:362–73.
 35. Sugimoto K, Lee DH, Lee JY, Yu SJ, Moriyasu F, Sakamaki K, et al. Multiparametric US for identifying patients with high-risk NASH: A derivation and validation study. *Radiology.* 2021;301:625–34.
 36. Perumpail BJ, Khan MA, Yoo ER, Cholankeril G, Kim D, Ahmed A. Clinical epidemiology and disease burden of nonalcoholic fatty liver disease. *World J Gastroenterol.* 2017;23:8263–76.

How to cite this article: Li J, Lu X, Zhu Z, Kalutkiewicz KJ, Mounajjed T, Therneau TM, et al. Head-to-head comparison of magnetic resonance elastography-based liver stiffness, fat fraction, and T1 relaxation time in identifying at-risk NASH. *Hepatology.* 2023;78:1200–1208. <https://doi.org/10.1097/HEP.0000000000000417>